US008344937B2

(12) **United States Patent**
Drake et al.

(10) **Patent No.: US 8,344,937 B2**
(45) **Date of Patent: Jan. 1, 2013**

(54) **METHODS AND APPARATUS FOR INTEGRATION OF DISTRIBUTED SENSORS AND AIRPORT SURVEILLANCE RADAR TO MITIGATE BLIND SPOTS**

(75) Inventors: **Peter R. Drake**, Northborough, MA (US); **Yuchoi F. Lok**, Framingham, MA (US)

(73) Assignee: **Raytheon Company**, Waltham, MA (US)

(*) Notice: Subject to any disclaimer, the term of this patent is extended or adjusted under 35 U.S.C. 154(b) by 358 days.

(21) Appl. No.: **12/761,590**

(22) Filed: **Apr. 16, 2010**

(65) **Prior Publication Data**

US 2010/0265120 A1 Oct. 21, 2010

Related U.S. Application Data

(60) Provisional application No. 61/170,250, filed on Apr. 17, 2009, provisional application No. 61/226,884, filed on Jul. 20, 2009.

(51) **Int. Cl.**
G01S 13/72 (2006.01)

(52) **U.S. Cl.** ..... **342/36**; 342/59; 342/26 R; 342/159; 342/90; 342/95

(58) **Field of Classification Search** ..... 342/36, 342/59, 26 R, 26 D, 159, 90, 95–97
See application file for complete search history.

(56) **References Cited**

U.S. PATENT DOCUMENTS

3,448,450	A	6/1969	Alfandari et al.	
4,961,075	A	10/1990	Ward	
6,215,438	B1	4/2001	Oswald et al.	
6,653,971	B1	11/2003	Guice et al.	
7,006,038	B2	2/2006	Smith	
7,675,458	B2 *	3/2010	Hubbard et al.	342/159
7,864,103	B2 *	1/2011	Weber et al.	342/123
7,948,429	B2 *	5/2011	Drake et al.	342/26 R
8,115,333	B2 *	2/2012	Parsche et al.	290/55
8,217,828	B2 *	7/2012	Kirk	342/62
8,253,621	B1 *	8/2012	Friesel	342/95
2001/0033246	A1	10/2001	Burchett et al.	
2002/0024652	A1 *	2/2002	Ooga	356/28.5
2004/0119633	A1	6/2004	Oswald et al.	
2007/0024494	A1 *	2/2007	Dizaji et al.	342/90
2008/0266171	A1 *	10/2008	Weber et al.	342/123

(Continued)

FOREIGN PATENT DOCUMENTS

EP 1345044 A1 9/2003

(Continued)

OTHER PUBLICATIONS

Notification of Transmittal of the International Search Report and the Written Opinion of the International Searching Authority, or the Declaration, PCT/US2009/042789 dated Aug. 25, 2009.

(Continued)

Primary Examiner — John B Sotomayor
(74) *Attorney, Agent, or Firm* — Daly, Crowley, Mofford & Durkee, LLP

(57) **ABSTRACT**

Methods and apparatus for a first radar; identifying a blind spot in coverage of the first radar; providing a second radar to illuminate the blind spot, and merging data from the first and second radars using target classification prior to tracking to reduce false targets. In one embodiment, polarimetric data is used to classify targets.

15 Claims, 16 Drawing Sheets

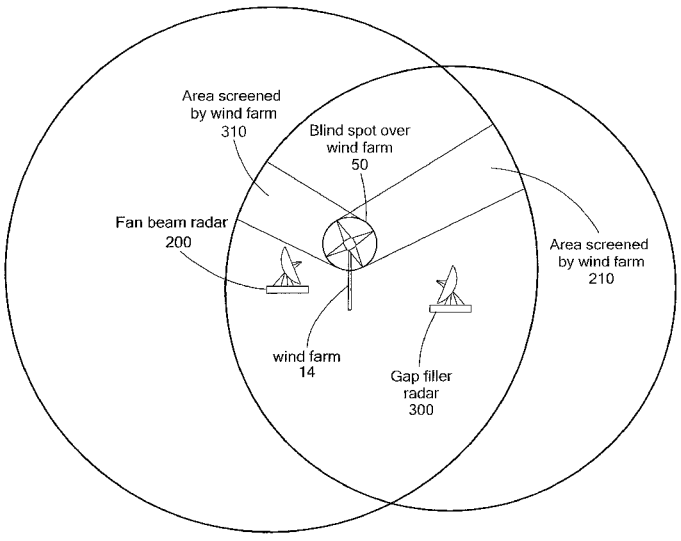

U.S. PATENT DOCUMENTS

2009/0202347	A1*	8/2009	Rugger	416/31
2010/0079328	A1*	4/2010	Drake et al.	342/36
2010/0265120	A1*	10/2010	Drake et al.	342/36
2011/0181455	A1*	7/2011	Vanuytven	342/27
2011/0260908	A1*	10/2011	New et al.	342/59

FOREIGN PATENT DOCUMENTS

GB	1100119		1/1968
GB	0701869.0		1/2007
GB	0710209.8		5/2007
GB	2439204	A	12/2007
GB	0710209.8		5/2008
GB	2447560	A	9/2008
GB	2448488	A	10/2008
GB	0813679.8		2/2009
GB	2439205	B	4/2009
GB	2441053	B	4/2009
GB	2453121	A	4/2009
GB	2447560	A	7/2009
GB	2447560	B	10/2009
GB	2461848	A	1/2010
GB	2461849	A	1/2010
GB	2461850	A	1/2010
GB	2461851	A	1/2010
WO	WO 9800729		1/1998
WO	WO 0003264	A1	1/2000
WO	WO 0159473	A2	8/2001
WO	WO 0159473	A3	8/2001
WO	WO 2008001092	A2	1/2008
WO	WO 2008001092	A3	1/2008
WO	WO 2008093036	A2	8/2008
WO	WO 2008093036	A3	8/2008
WO	WO 2008093092	A2	8/2008
WO	WO 2008093092	A3	8/2008
WO	WO 2008/145993		12/2008
WO	WO 2008145993	A2	12/2008
WO	WO 2010028831	A1	3/2010

OTHER PUBLICATIONS

Written Opinion of the International Searching Authority, PCT/US2009/042789 dated Aug. 25, 2009.

U.S. Appl. No. 12/435,508, filed May 5, 2009.

Notification of Transmittal of the International Search Report and the Written Opinion of the International Searching Authority, or the Declaration, PCT/US2010/031372 dated Jul. 19, 2010, 6 pages.

Written Opinion of the International Searching Authority, PCT/US2010/031372 dated Jul. 19, 2010, 11 pages.

Jackson, C.A.; Butler, M.M.: "Options for mitigation of the effects of windfarms on radar systems", Radar Systems, 2007 IET International Conference OON, Oct. 18, 2007, XP007913802, ISSN: 0537-9989, ISBN: 978-0-86341-848-8, 6 pages.

Bannister, David J.: "Radar in-fill for Greater Wash area—Feasibility study final report", Aug. 31, 2007, XP007913816, Retrieved from the Internet: URL:http://www.bwea.com/pdf/AWG_Reference/0709%20BERR%20COWRIE%20Radar%20in-fill%20for%20Greater%20Wash%20area%20-%20Feasibility%20study%20final%20report.pdf, 41 pages.

Raytheon Canada Ltd.: "Report on advanced mitigating techniques to remove the effects of wind turbines and wind farms on the Raytheon ASR-10/23SS Radars", Jul. 17, 2006, XP007913794, Retrieved from the Internet: URL:http://www.decc.gov.uk/assets/decc/what%20we%20do%20uk%20energy%20supply/energy%20mix/renewable%20energy/planning/on_off_wind/aero_military/file37012.pdf_and_file37014.pdf, 98 pages.

Auld: "Options for mitigating the impact of wind turbines on NERL's primary radar infrastructure" 2006, XP007913817, Retrieved from the internet: URL:http://www.bwea.com/pdf/AWG_Reference/0701%20BERR%20Options%20for%20mitigating%20the%20impacts%20of%20wind%20turbines%20on%20NERL%27s%20primary%20radar%20infrastructure.pdf, 11 pages.

Perry, J. et al.: "Wind Farm Clutter Mitigation in Air Surveillance Radar", Radar Conference, 2007 IEEE, IEEE, PI LNKD—DOI:10.1109/RADAR.2007.374197, Apr. 1, 2007, XP031180885, ISBN: 978-1-4244-0283-0, 6 pages.

Craig Webster, "Wind farms vs. radar—seeing through the clutter", Cambridge Consultants, Innovation Day 2008, Oct. 22, 2008, 29 pages.

Notice of Allowance and Issue Fee due for U.S. Appl. No. 12/435,508, filed May 5, 2009, 17 pages.

Notification Concerning Transmittal of International Preliminary Report on Patentability (Chapter 1 of the Patent Cooperation Treaty), PCT/US2010/031372, date of mailing Oct. 27, 2011, 11 pages.

* cited by examiner

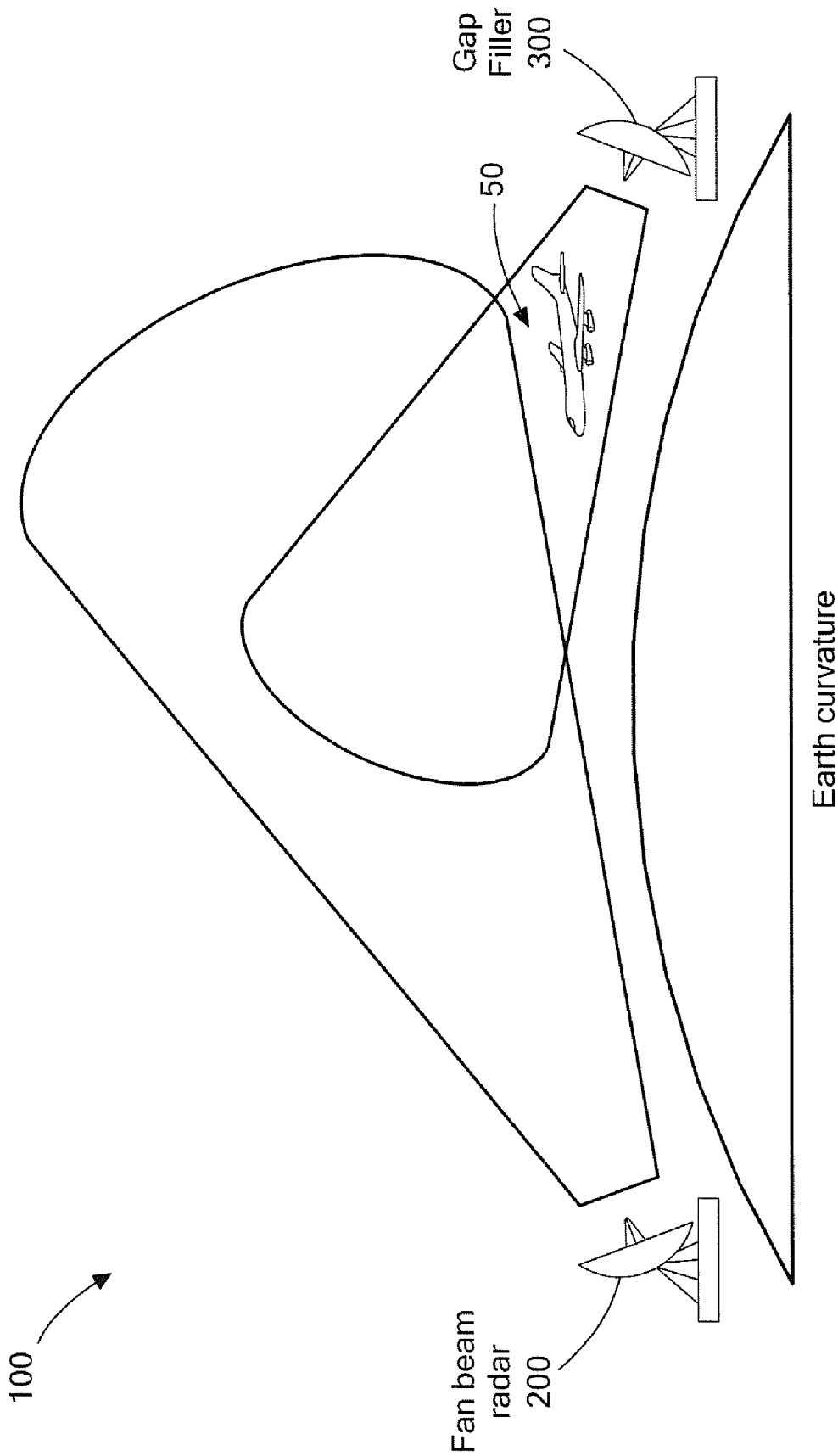

FIG. 1

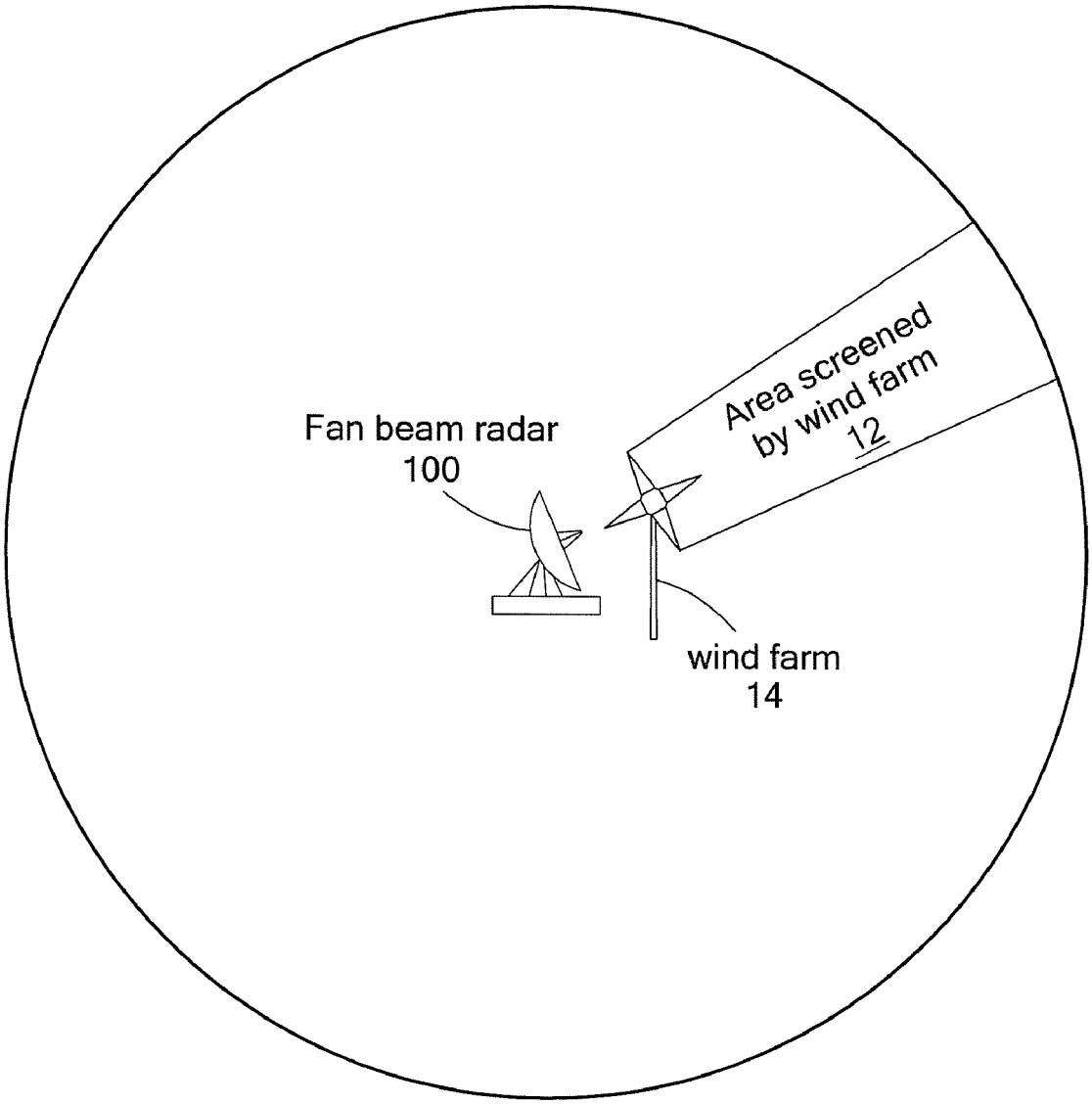

FIG. 2

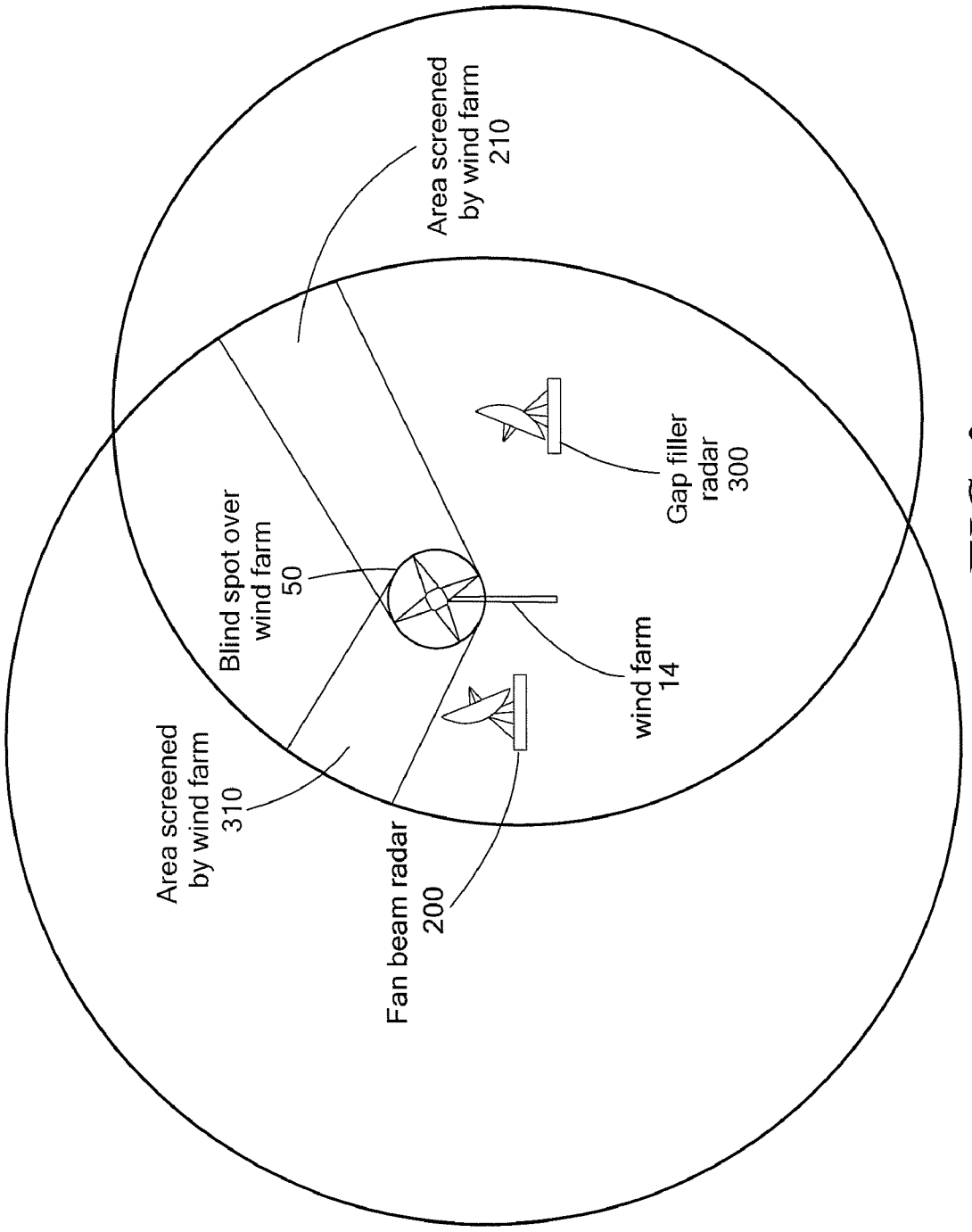
Area screened by wind farm 210
Gap filler radar 300
Blind spot over wind farm 50
wind farm 14
Area screened by wind farm 310
Fan beam radar 200

FIG. 3

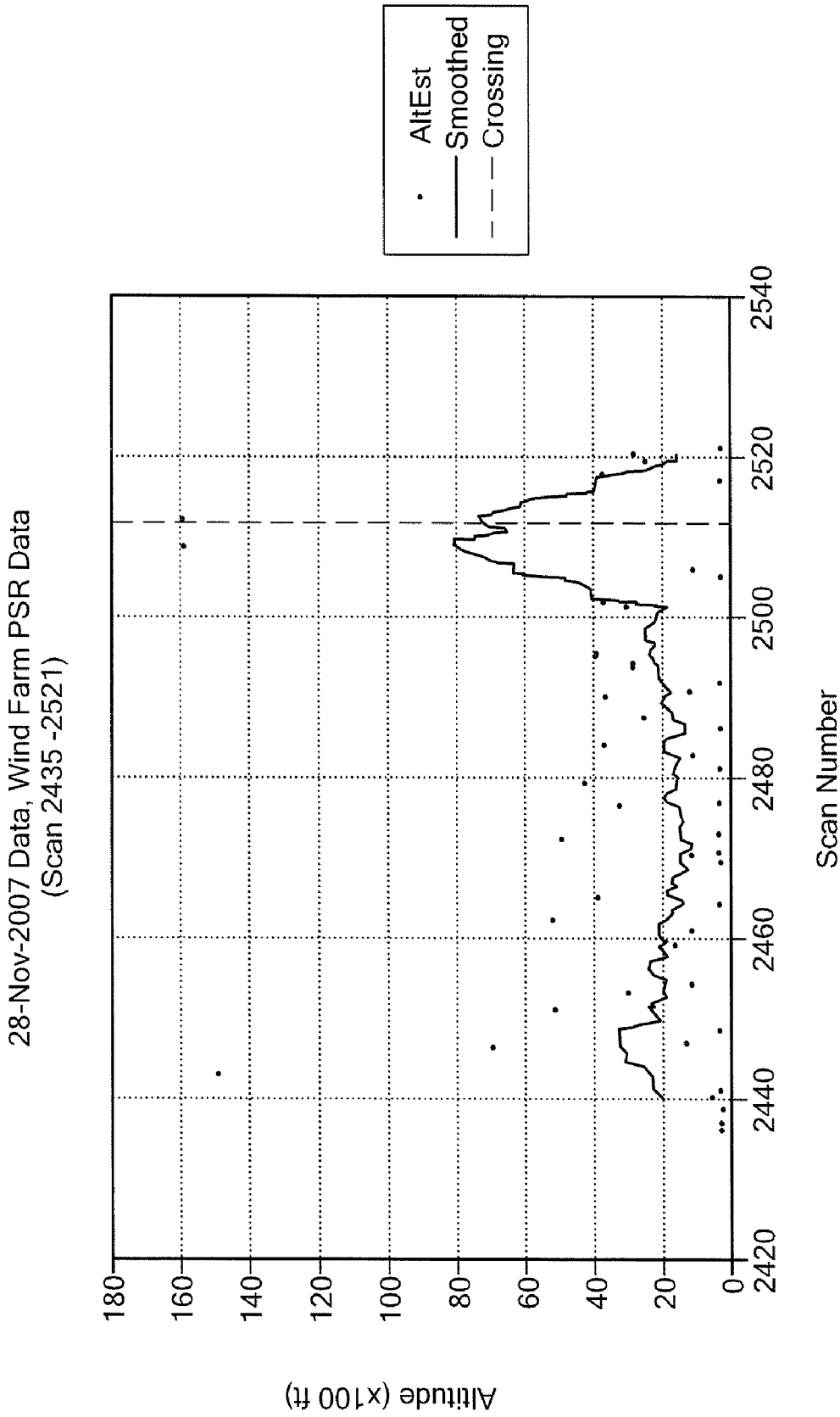
28-Nov-2007 Data, Wind Farm PSR Data
(Scan 2435 -2521)
AltEst
Smoothed
Crossing
Altitude (x100 ft)
0
20
40
60
80
100
120
140
160
180
2420
2440
2460
2480
2500
2520
2540
Scan Number

FIG. 4

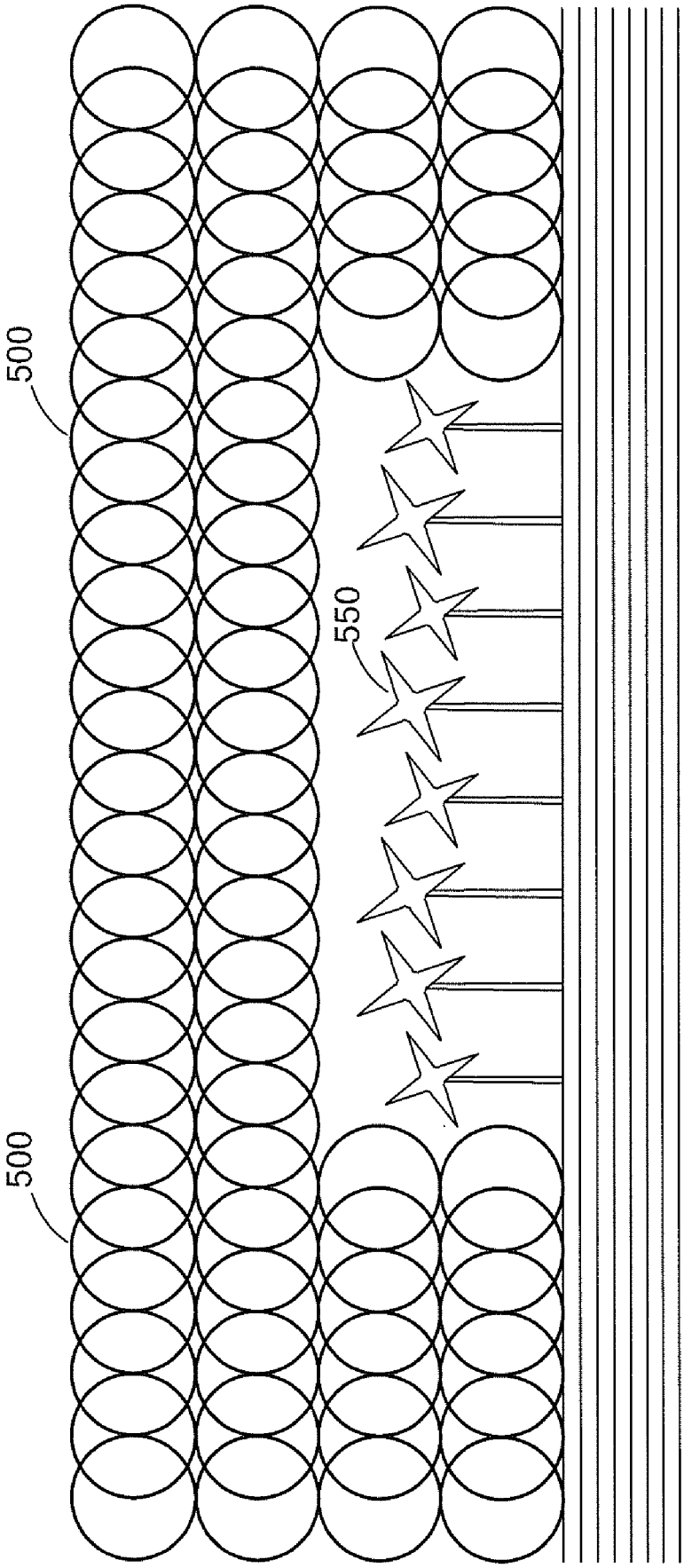

FIG. 5

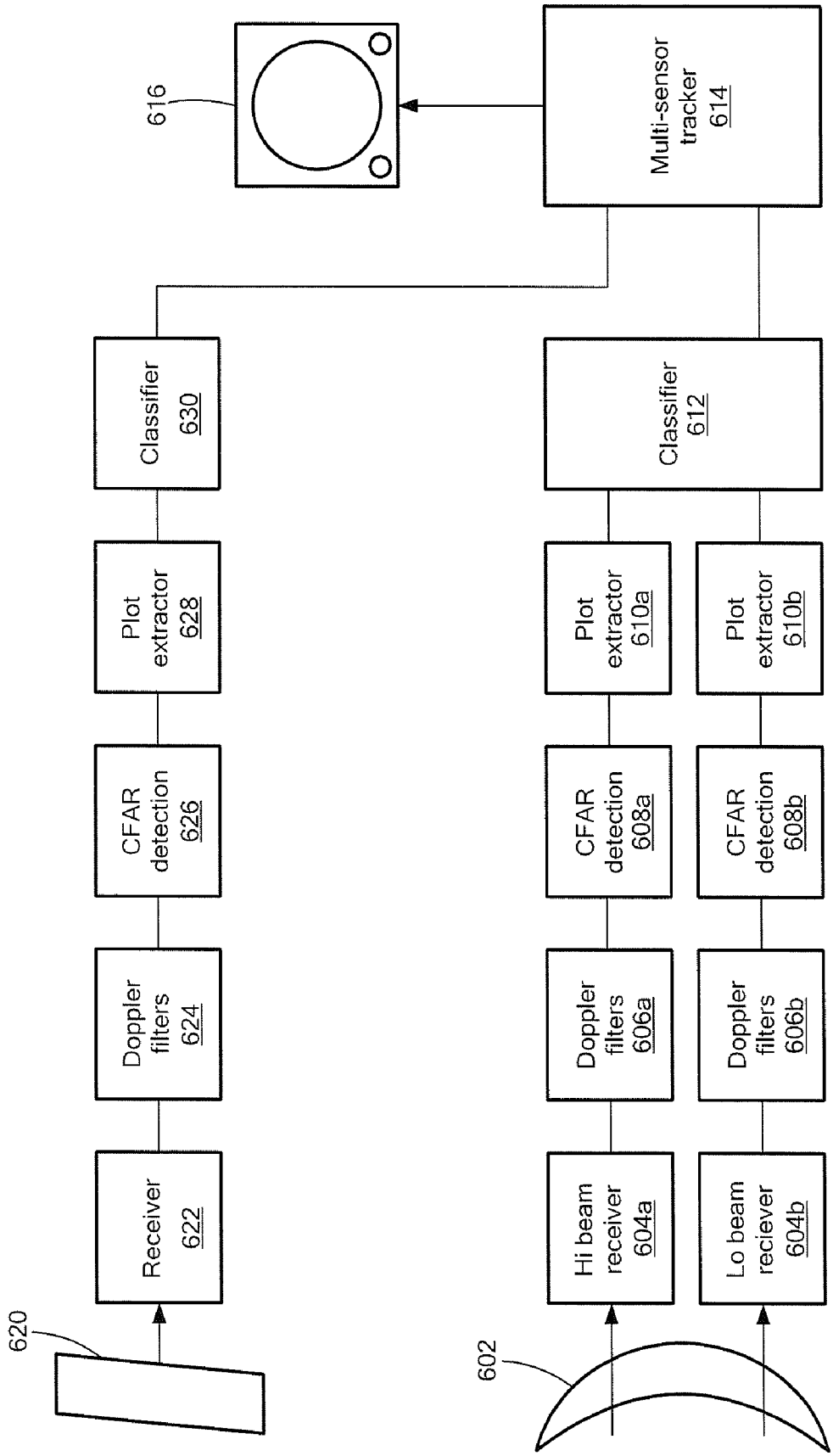
616
Multi-sensor tracker 614
Classifier 630
Classifier 612
Plot extractor 628
Plot extractor 610a
Plot extractor 610b
CFAR detection 626
CFAR detection 608a
CFAR detection 608b
Doppler filters 624
Doppler filters 606a
Doppler filters 606b
Receiver 622
Hi beam receiver 604a
Lo beam reciever 604b
620
602

FIG. 6

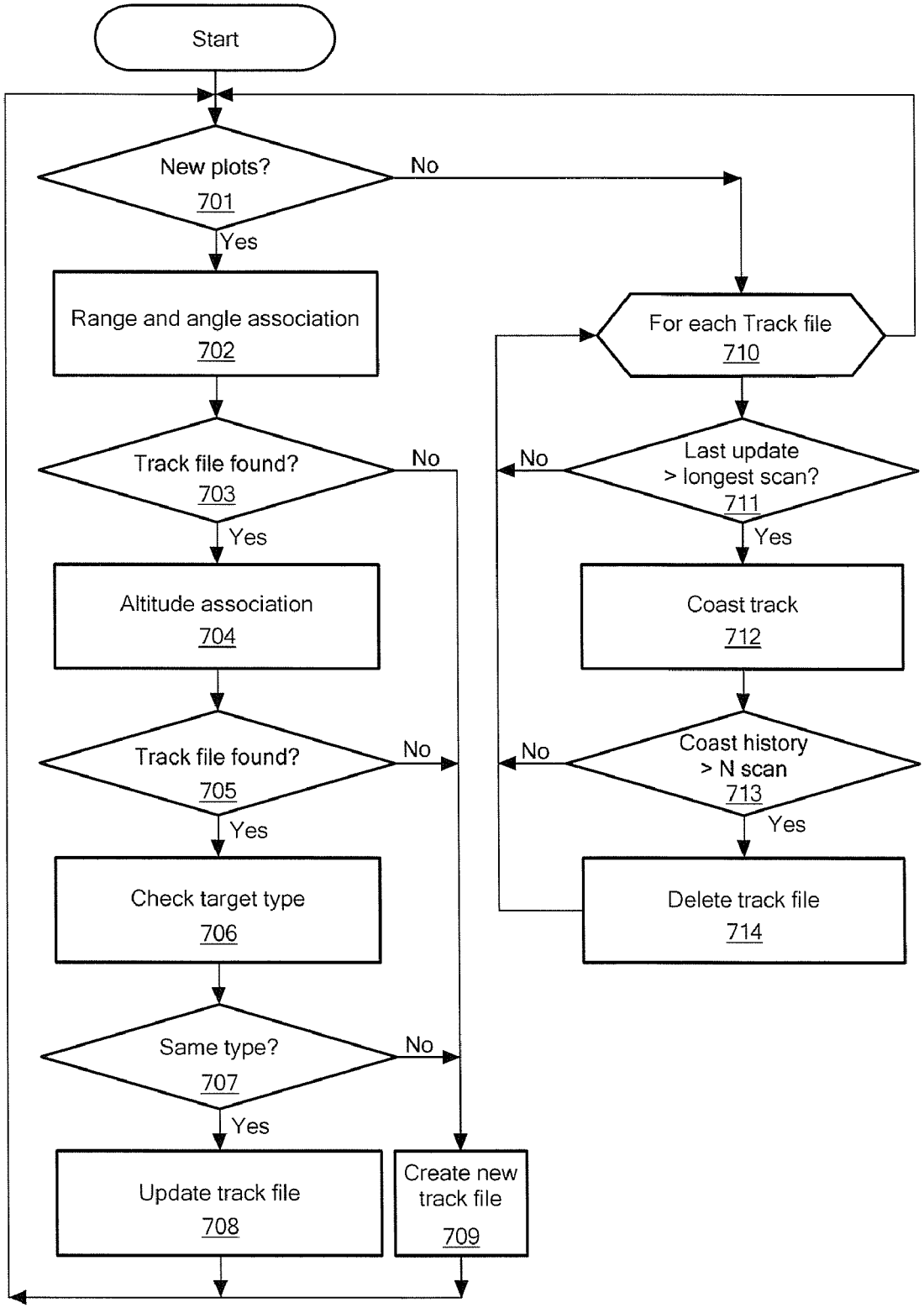
Start
New plots?
701
No
Yes
Range and angle association
702
Track file found?
703
No
Yes
Altitude association
704
Track file found?
705
No
Yes
Check target type
706
Same type?
707
No
Yes
Update track file
708
Create new track file
709
For each Track file
710
Last update > longest scan?
711
No
Yes
Coast track
712
Coast history > N scan
713
No
Yes
Delete track file
714

FIG. 7

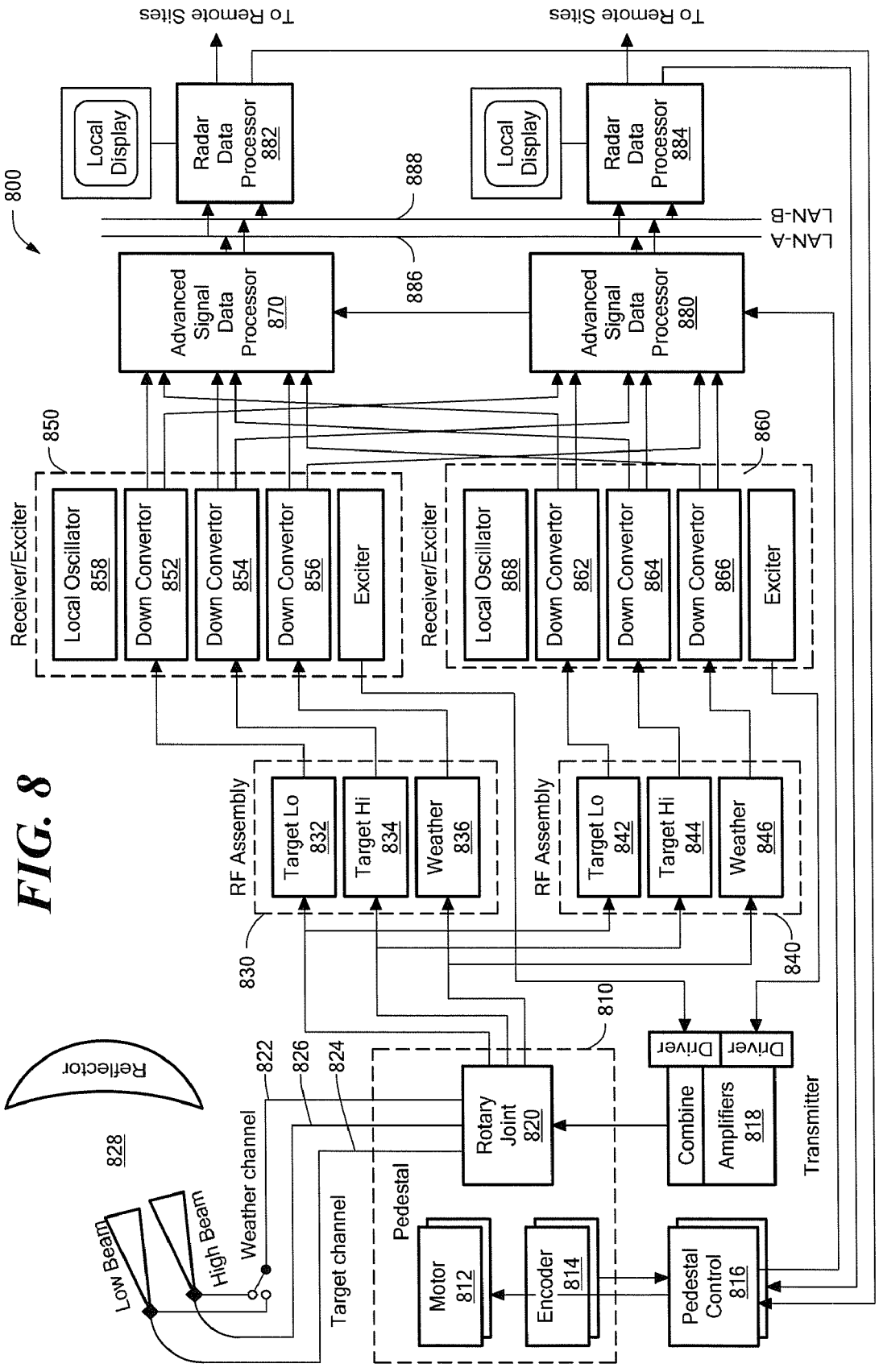
800
To Remote Sites
To Remote Sites
Local Display
Radar Data Processor 882
Local Display
Radar Data Processor 884
888
LAN-B
LAN-A
886
Advanced Signal Data Processor 870
Advanced Signal Data Processor 880
850
860
Receiver/Exciter
Local Oscillator 858
Down Convertor 852
Down Convertor 854
Down Convertor 856
Exciter
Receiver/Exciter
Local Oscillator 868
Down Convertor 862
Down Convertor 864
Down Convertor 866
Exciter
RF Assembly
Target Lo 832
Target Hi 834
Weather 836
RF Assembly
Target Lo 842
Target Hi 844
Weather 846
830
840
810
Driver
Driver
Combine
Amplifiers 818
Transmitter
Reflector
828
822
826
824
Rotary Joint 820
Pedestal
Low Beam
High Beam
Weather channel
Target channel
Motor 812
Encoder 814
Pedestal Control 816

FIG. 8

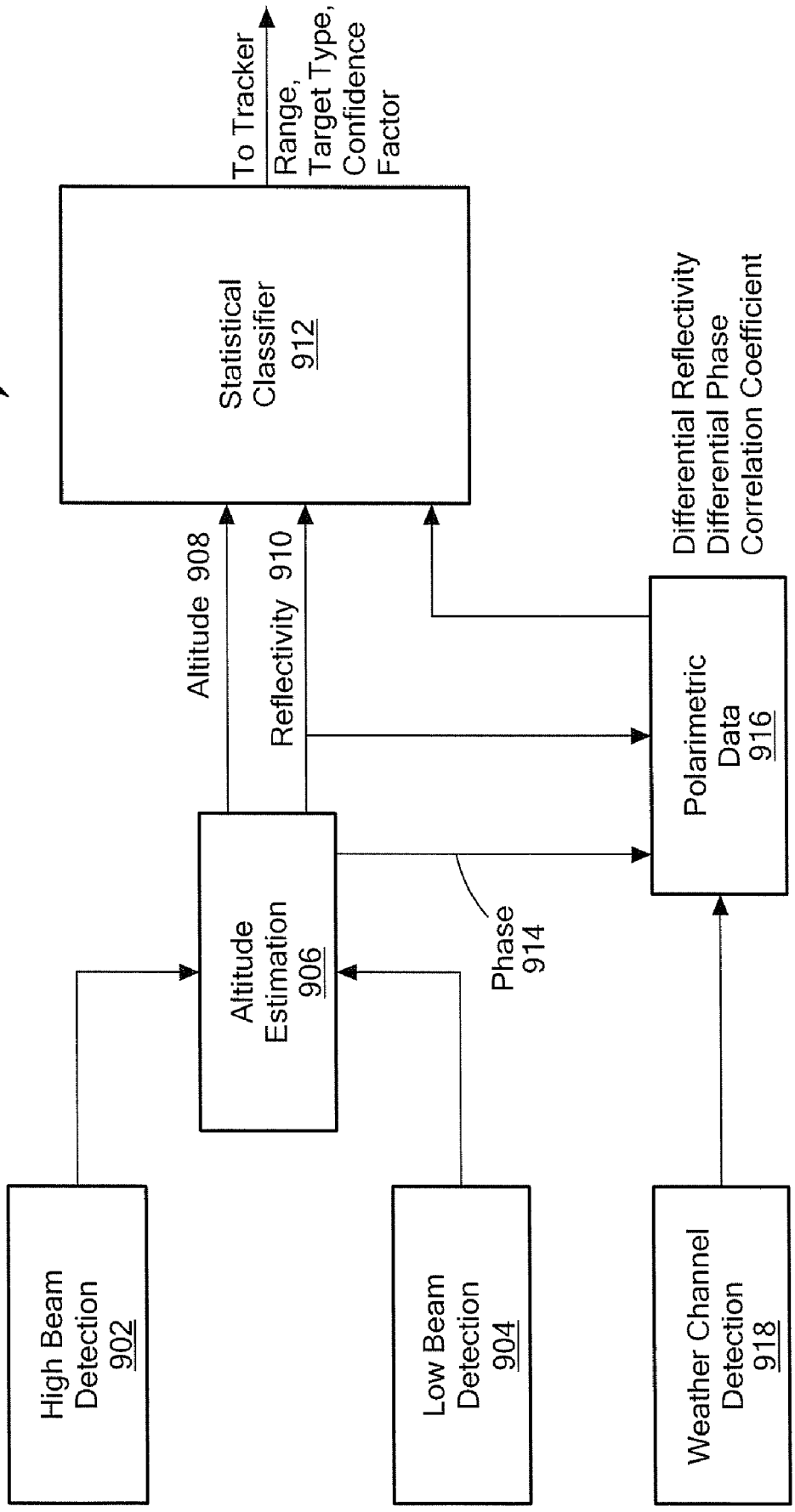
900
Statistical Classifier 912
To Tracker
Range, Target Type, Confidence Factor
Altitude 908
Reflectivity 910
Differential Reflectivity
Differential Phase
Correlation Coefficient
Polarimetric Data 916
Altitude Estimation 906
Phase 914
High Beam Detection 902
Low Beam Detection 904
Weather Channel Detection 918

FIG. 9

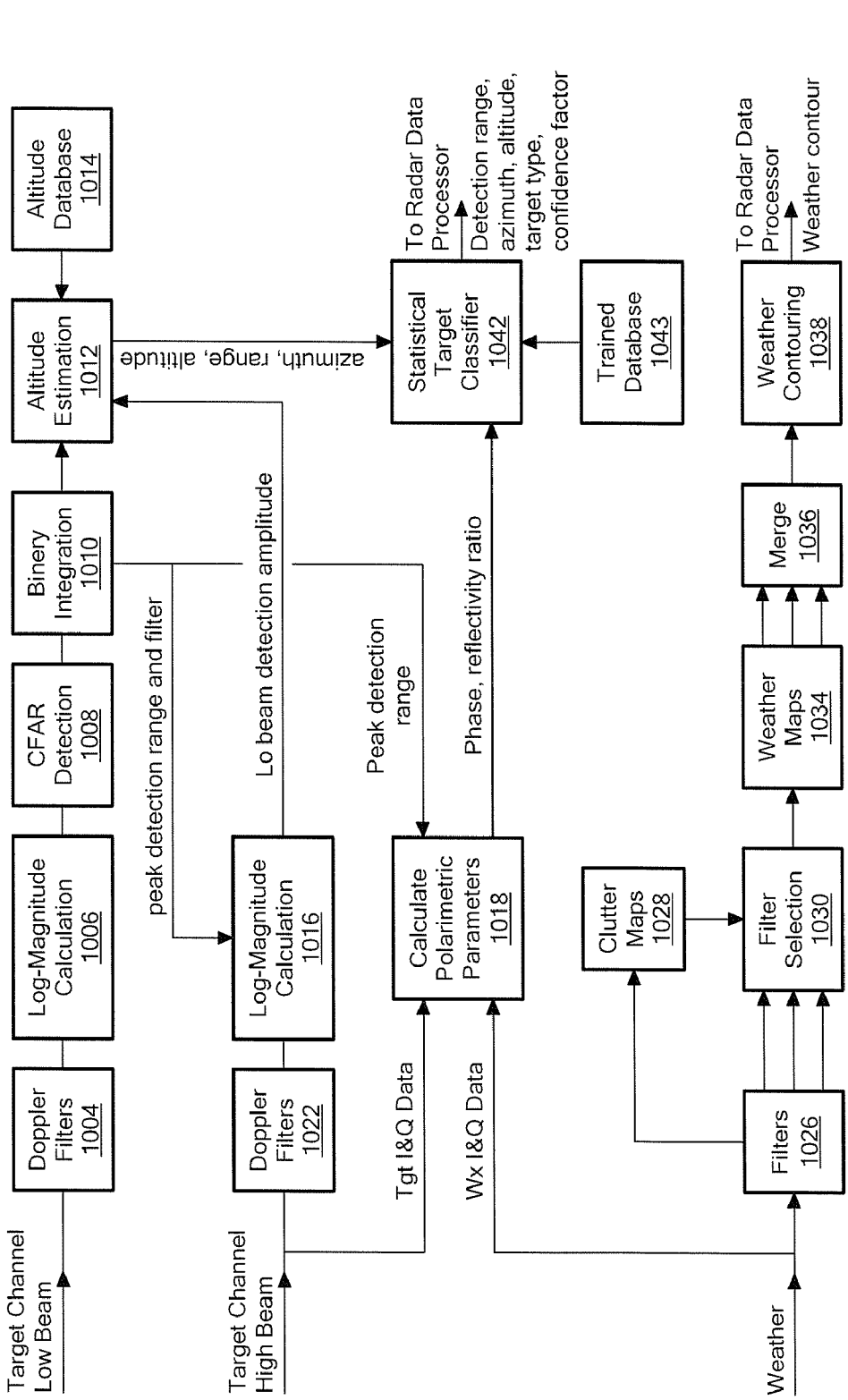
1000
Altitude Database 1014
Altitude Estimation 1012
Binery Integration 1010
CFAR Detection 1008
Log-Magnitude Calculation 1006
Doppler Filters 1004
Target Channel Low Beam
azimuth, range, altitude
peak detection range and filter
Lo beam detection amplitude
Peak detection range
Phase, reflectivity ratio
Statistical Target Classifier 1042
To Radar Data Processor
Detection range, azimuth, altitude, target type, confidence factor
Trained Database 1043
Log-Magnitude Calculation 1016
Doppler Filters 1022
Target Channel High Beam
Tgt I&Q Data
Calculate Polarimetric Parameters 1018
Wx I&Q Data
Clutter Maps 1028
Filter Selection 1030
Filters 1026
Weather
Weather Maps 1034
Merge 1036
Weather Contouring 1038
To Radar Data Processor
Weather contour

FIG. 10

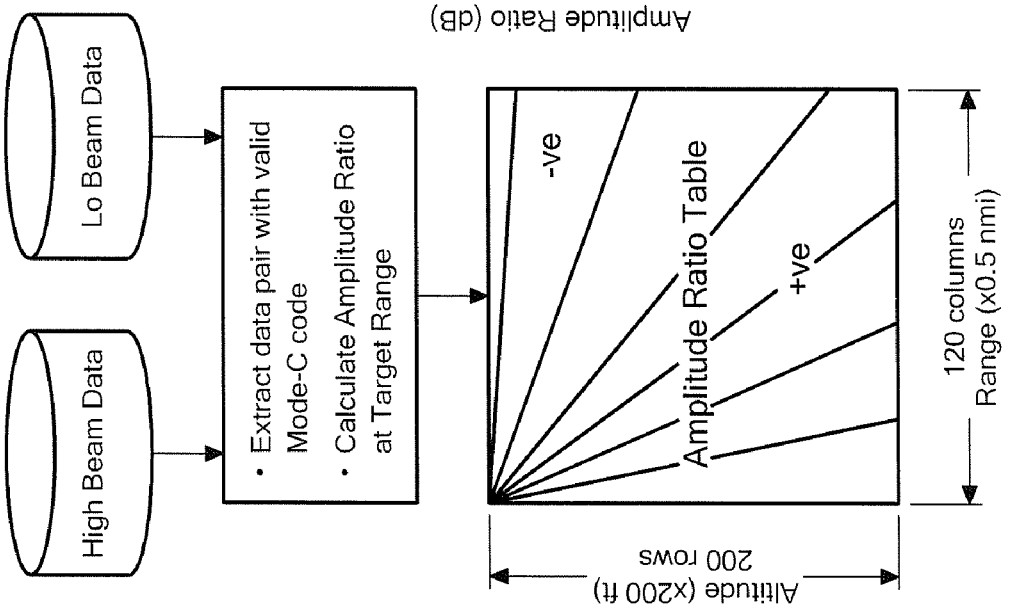

FIG. 11A

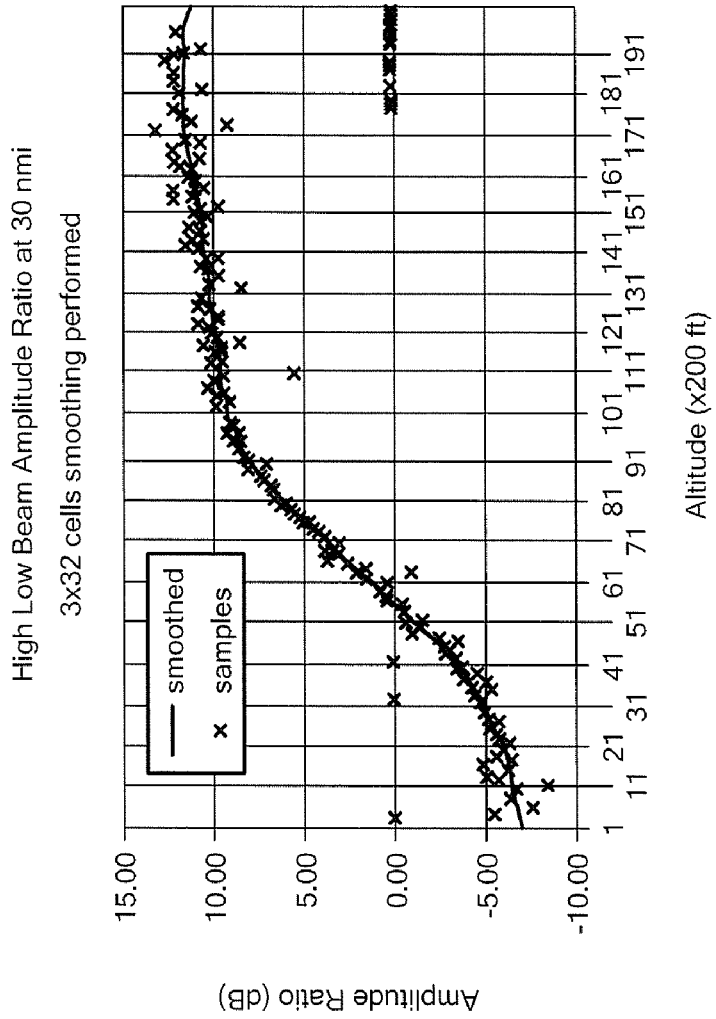

FIG. 11B

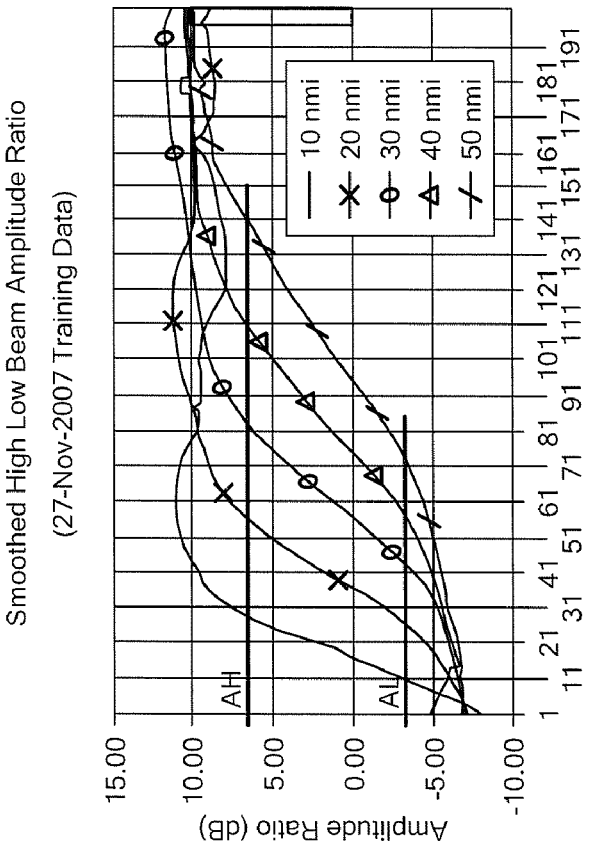

FIG. 12A

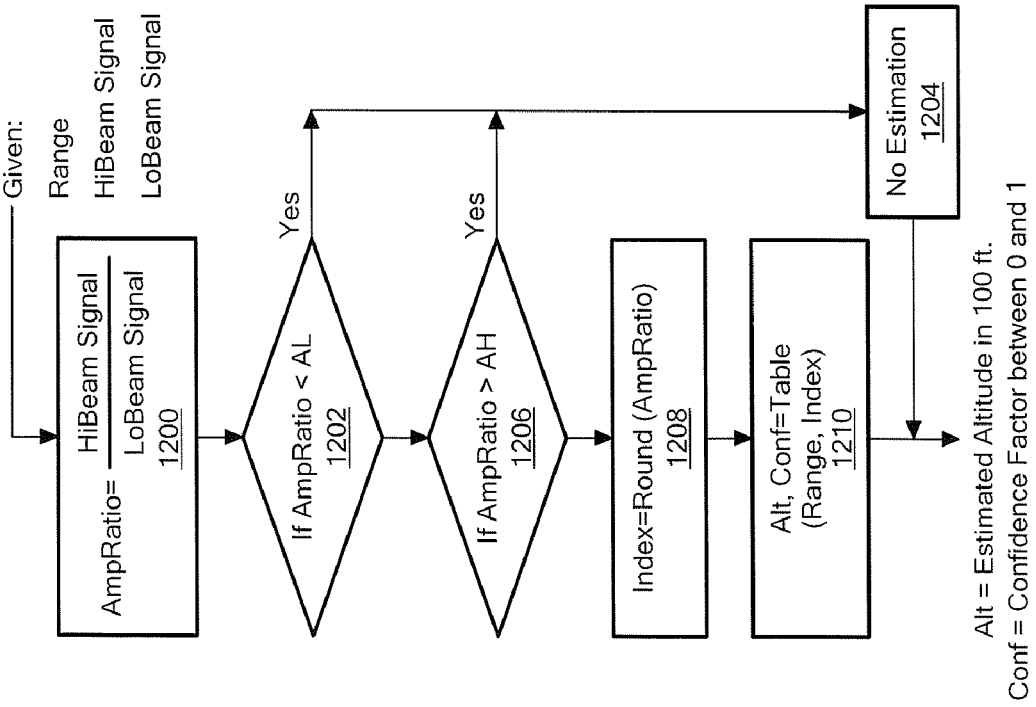

FIG. 12

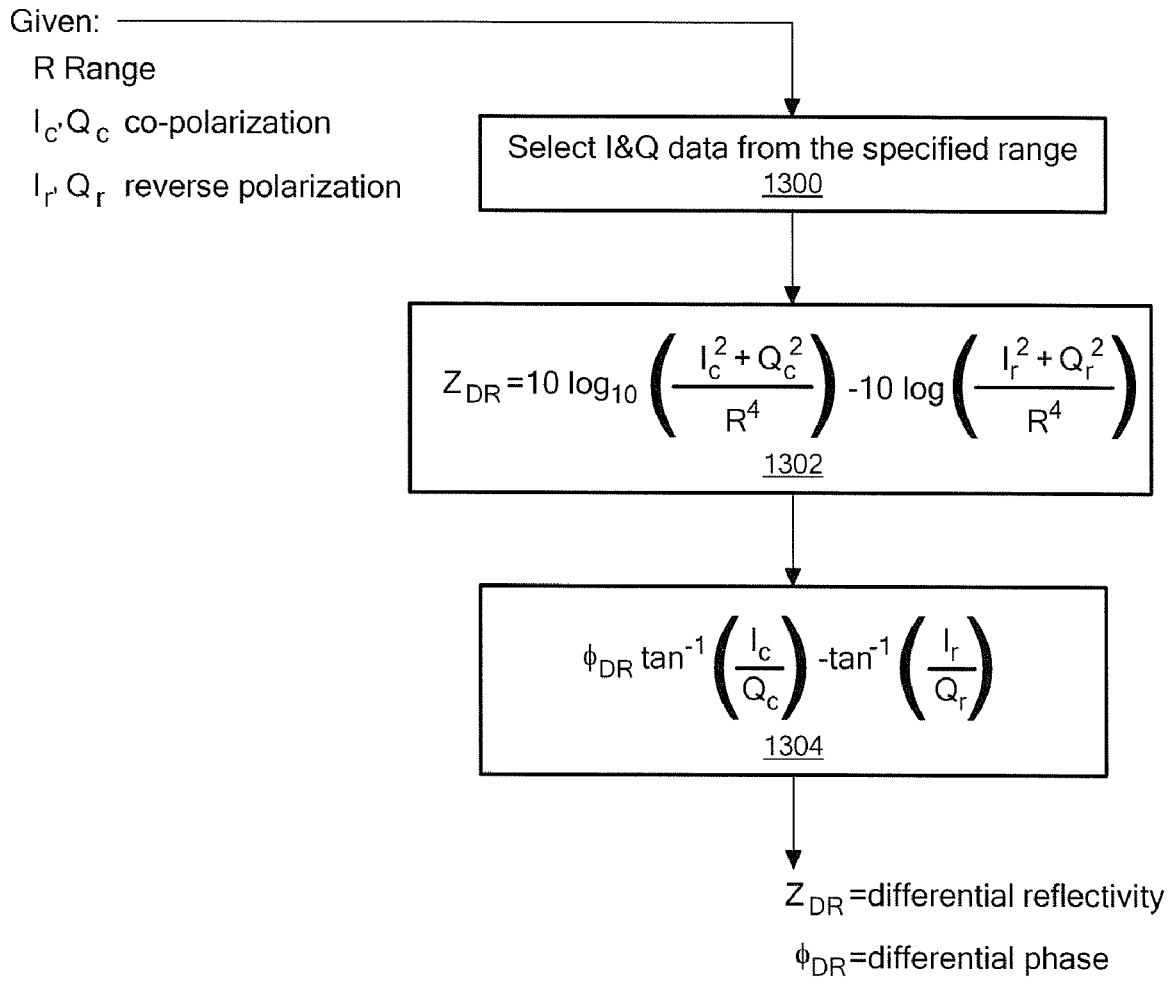
Given:
R Range
I_c, Q_c co-polarization
I_r, Q_r reverse polarization
Select I&Q data from the specified range
1300
$Z_{DR}=10 \log_{10}\left(\frac{I_c^2+Q_c^2}{R^4}\right)-10 \log\left(\frac{I_r^2+Q_r^2}{R^4}\right)$
1302
$\phi_{DR} \tan^{-1}\left(\frac{I_c}{Q_c}\right)-\tan^{-1}\left(\frac{I_r}{Q_r}\right)$
1304
Z_{DR}=differential reflectivity
ϕ_{DR}=differential phase

FIG. 13

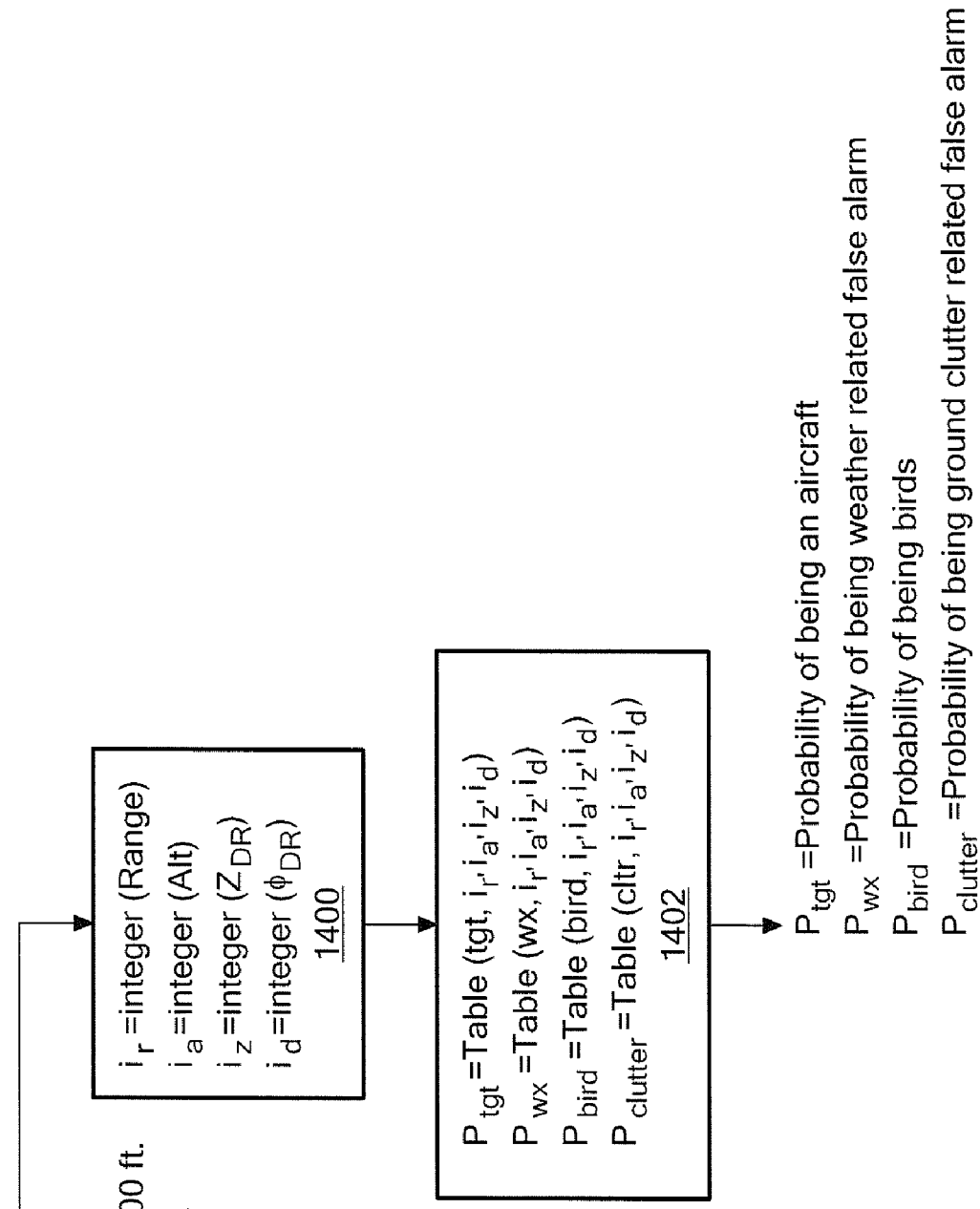
Given:
Range
Alt=Estimated Altitude in 100 ft.
Z_{DR} =differential reflectivity
ϕ_{DR} =differential phase
i_r =integer (Range)
i_a =integer (Alt)
i_z =integer (Z_{DR})
i_d =integer (ϕ_{DR})
1400
P_{tgt} =Table (tgt, i_r, i_a, i_z, i_d)
P_{wx} =Table (wx, i_r, i_a, i_z, i_d)
P_{bird} =Table (bird, i_r, i_a, i_z, i_d)
$P_{clutter}$ =Table (cltr, i_r, i_a, i_z, i_d)
1402
P_{tgt} =Probability of being an aircraft
P_{wx} =Probability of being weather related false alarm
P_{bird} =Probability of being birds
$P_{clutter}$ =Probability of being ground clutter related false alarm

FIG. 14

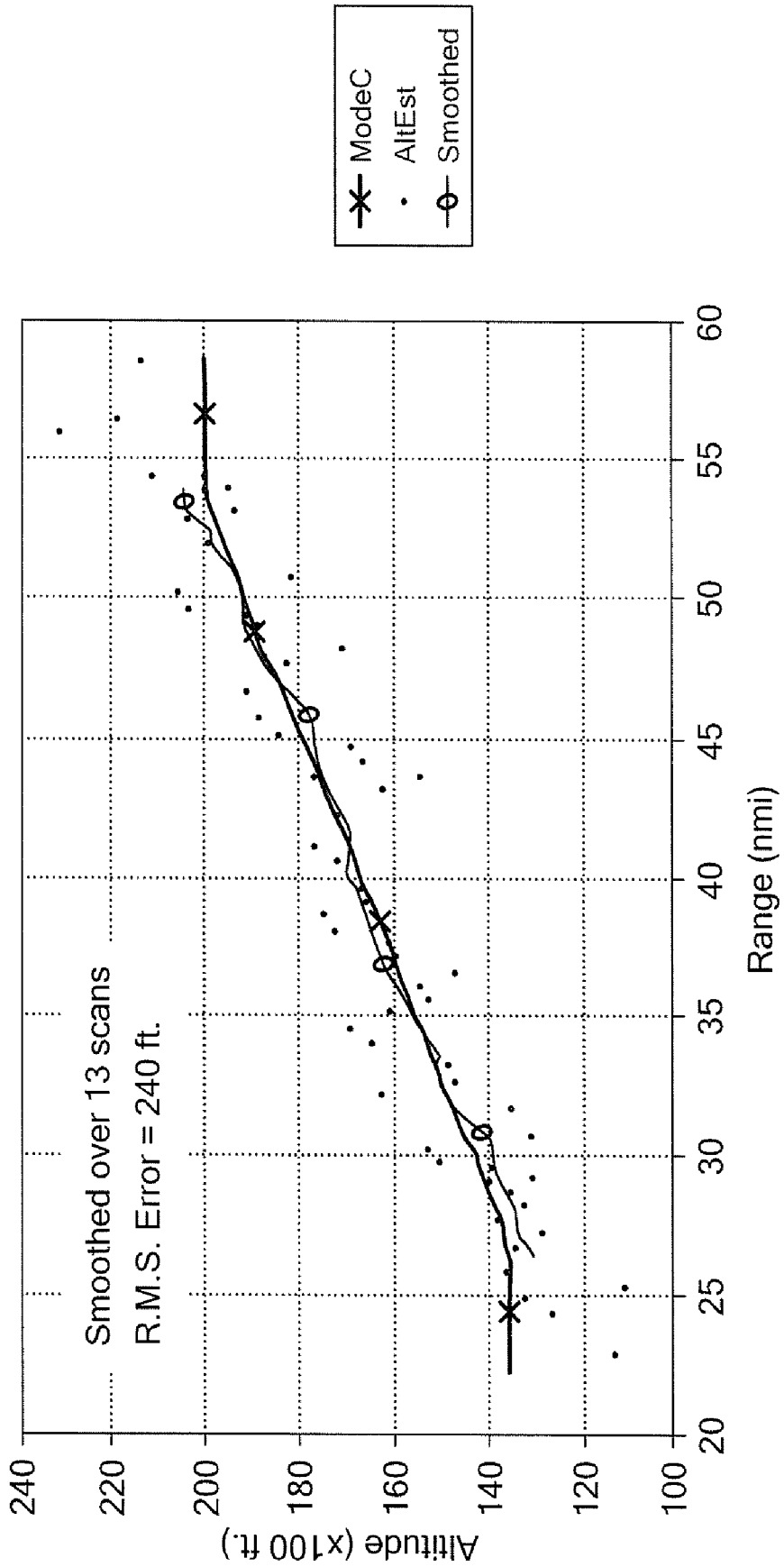
ModeC
AltEst
Smoothed
Smoothed over 13 scans
R.M.S. Error = 240 ft.
Altitude (x100 ft.)
Range (nmi)
240
220
200
180
160
140
120
100
20
25
30
35
40
45
50
55
60

FIG. 15

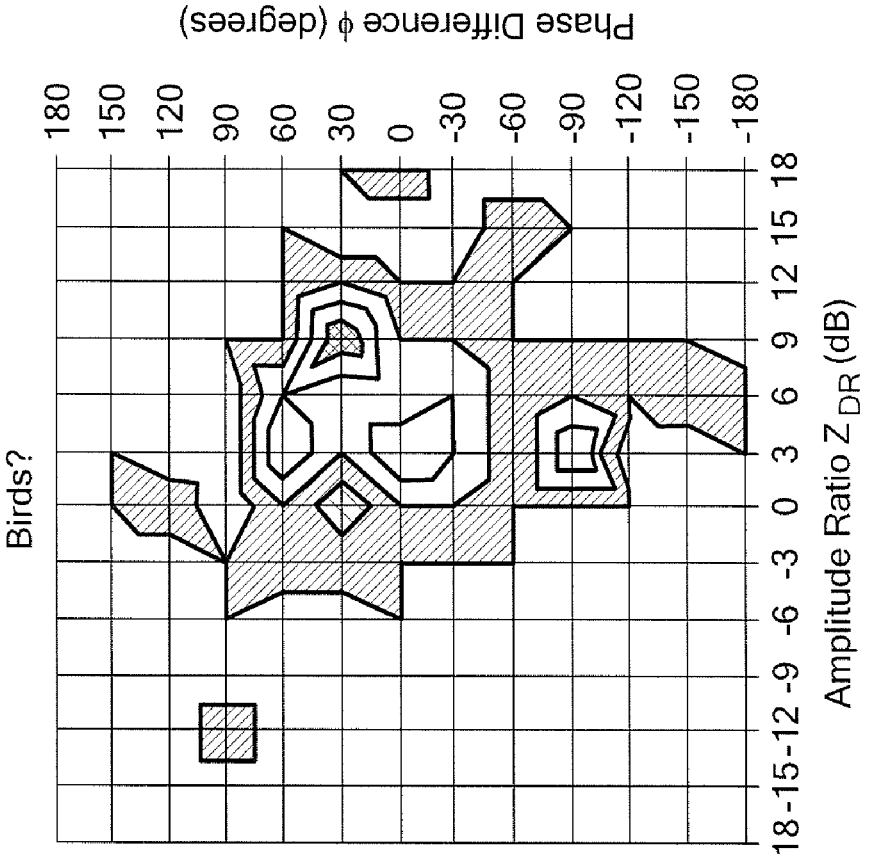
Birds?
Phase Difference ϕ (degrees)
180 150 120 90 60 30 0 -30 -60 -90 -120 -150 -180
-18 -15 -12 -9 -6 -3 0 3 6 9 12 15 18
Amplitude Ratio Z_{DR} (dB)

FIG. 17

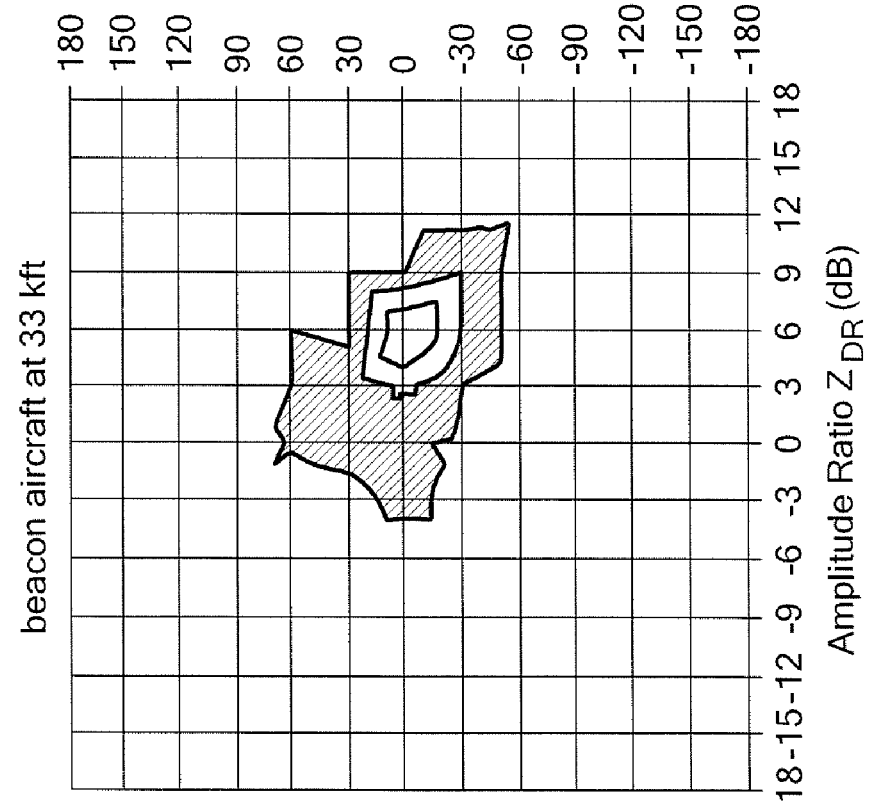
beacon aircraft at 33 kft
Phase Difference ϕ (degrees)
180 150 120 90 60 30 0 -30 -60 -90 -120 -150 -180
-18 -15 -12 -9 -6 -3 0 3 6 9 12 15 18
Amplitude Ratio Z_{DR} (dB)

FIG. 16

METHODS AND APPARATUS FOR INTEGRATION OF DISTRIBUTED SENSORS AND AIRPORT SURVEILLANCE RADAR TO MITIGATE BLIND SPOTS

CROSS REFERENCE TO RELATED APPLICATIONS

The present application claims the benefit of U.S. Provisional Patent Application No. 61/170,250, filed on Apr. 17, 2009, and U.S. Provisional Patent Application No. 61/226,884, filed on Jul. 20, 2009, which are both incorporated herein by reference.

STATEMENT REGARDING FEDERALLY SPONSORED RESEARCH

This invention was made with Government support under Contract F19628-96-D-0038 awarded by the US Air Force. The Government may have certain rights in the invention.

BACKGROUND

As is known in the art, there are a number of significant blind spots for certain types of radars. For example, blinds spots can be due to terrain obstruction and/or Earth curvature, man-made objects, such wind farms, and interference created by wind farms. Such blind spots can significantly degrade radar performance.

SUMMARY

In one aspect of the invention, a method comprises employing a first radar, identifying a blind spot in coverage of the first radar, providing a second radar to illuminate the blind spot, and merging data from the first and second radars using target classification prior to tracking to reduce false targets.

The method can further include one or more of the following features: the blind spot is created by a wind farm, the first radar is an airport surveillance radar and the second radar is a gap filler radar, the gap filler radar is a pencil beam radar, the airport surveillance radar includes parallel paths for a high beam receiver and a low beam receiver, identifying false targets by one or more of: an altitude estimation of a target is low and is near the blind spot, which includes a wind farm area; an estimated radial velocity of the target does not match scan-to-scan movement; a wide Doppler spectrum fits the wind turbine profile; and the target is not detected by the second radar, which is a pencil-beam gap filler radar, identifying an aircraft target by detecting an altitude estimation drop due to interference by the wind farm that is higher than a predefined wind farm altitude; and/or detecting the target by the pencil-beam gap filler radar with an aircraft classification having a confidence factor greater than and is classified as aircraft with a confidence factor greater than a selected threshold, the target classification includes polarimetric characteristics, and the target classification includes at one or more of polarimetric characteristics, altitude estimation, detection cluster shape, and Doppler information.

In another aspect of the invention, a system comprises a first radar having a blind spot in coverage for the first radar, a second radar to illuminate the blind spot, and a tracker to merge data from the first and second radars using target classification prior to tracking to reduce false targets.

The system can further include one or more of the following features: the blind spot is created by a wind farm, the first radar is an airport surveillance radar and the second radar is a gap filler radar, the gap filler radar is a pencil beam radar, the airport surveillance radar includes parallel paths for a high beam receiver and a low beam receiver, the tracker identifies false targets by one or more of: an altitude estimation of a target is low and is near the blind spot, which includes a wind farm area; an estimated radial velocity of the target does not match scan-to-scan movement; a wide Doppler spectrum fits the wind turbine profile; and the target is not detected by the second radar, which is a pencil-beam gap filler radar, the tracker identifies an aircraft target by detecting an altitude estimation drop due to interference by the wind farm that is higher than a predefined wind farm altitude; and/or detecting the target by the pencil-beam gap filler radar with an aircraft classification having a confidence factor greater than and is classified as aircraft with a confidence factor greater than a selected threshold, the target classification includes polarimetric characteristics, and the target classification includes at one or more of polarimetric characteristics, altitude estimation, detection cluster shape, and Doppler information.

BRIEF DESCRIPTION OF THE DRAWINGS

The foregoing features of this invention, as well as the invention itself, may be more fully understood from the following description of the drawings in which:

FIG. **1** is a pictorial representation of a system having an airport surveillance radar and a gap filler radar;

FIG. **2** is a pictorial representation of an airport surveillance radar with a blind spot caused by a wind farm;

FIG. **3** is a schematic representation of system including gap filler radar to illuminate blind spots in an airport surveillance radar caused by a wind farm;

FIG. **4** is a graphical depiction of the estimated plot altitude on the wind farm is averaged to about 2,000 ft; when an aircraft flew over the wind farm at 16,000 ft, the resultant estimated altitude became 7,000 ft;

FIG. **5** is a pictorial representation of a pencil beam gap filler radar illuminating a blind spot and avoiding a wind farm;

FIG. **6** is a schematic representation showing processing modules in an airport surveillance radar and a gap filler radar;

FIG. **7** is a high level flowchart showing the Multi-sensor Tracker process.

FIG. **8** is a schematic representation of a system providing target classification;

FIG. **9** is a block diagram showing additional detail for the system of FIG. **8**;

FIG. **10** is a block diagram showing additional detail for the system of FIG. **9**;

FIG. **11** is a graphical representation of the method for generating the amplitude ratio versus altitude lookup table;

FIG. **12** is a flow diagram showing exemplary altitude estimating processing

FIG. **12**A is a graphical representation of smoothed high beam amplitude ratio data;

FIG. **13** is a flow diagram showing exemplary inphase and quadrature data processing;

FIG. **14** is a flow diagram of exemplary probability processing;

FIG. **15** is a graphical representation of altitude estimation versus range;

FIG. **16** is a mapping of amplitude ratio versus phase difference for an aircraft at 33 kft; and

FIG. **17** is a mapping of amplitude ratio versus phase difference for a possible bird migration.

DETAILED DESCRIPTION

FIG. **1** shows an exemplary system **100** including an airport surveillance radar (ASR) **200** and a relatively small phased

array, for example, radar **300**. The phased array radar **300** illuminates an area **50** under the field of view of the airport surveillance radar **200** resulting from curvature of the earth. As can be seen, the earth curvature creates a radar blind spot for the airport surveillance radar **200** that is addressed by the phased array radar **300**. As described below, data from the airport surveillance radar and the phased array radar can be merged to mitigate blind spots. It is understood that any practical number of radars, such as small phased array radars, can be added to illuminate desired areas and contribute data.

FIG. **2** shows a system including an airport surveillance radar **100** having a blind spot **12** due to a wind farm **14**. FIG. **3** shows an exemplary system including a fan beam airport surveillance radar **200** and a gap filler radar **300** that illuminates a blind spot **210** in the airport surveillance radar **200** created by a wind farm **14**. In similar way, the gap filler radar blind spot **310** is covered by the fan beam airport surveillance radar **200**. A blind spot **50** remains at the wind farm location.

The blind spot **50** is due to interference resulting from rotations of the individual wind turbines that create Doppler frequencies that the radar can detect as (false) moving targets. False targets may flood the wind farm area so that the radar detection mechanism may not be able to separate an aircraft flying over the wind farm from these false targets.

While conventional beam processing can estimate target altitude, false targets from the wind farm **14** will have low altitudes. When an aircraft is flying over the wind farm **14**, the resultant estimated altitude will be somewhere between the actual aircraft altitude and the wind farm altitude, as shown in FIG. **4**. Using the estimated altitude alone will not solve this type of blind spot in all cases. FIG. **4** shows that due to the limitation of the concurrent beam processing capability, the estimated plot altitude on the wind farm is averaged to about 2,000 ft. When an aircraft flew over the wind farm at 16,000 ft, the resultant estimated altitude became 7,000 ft.

In accordance with exemplary embodiments of the invention, merging data from a gap filler radar with an airport surveillance radar can mitigate blind spots. In one embodiment, a relatively low-cost phased array radar can be used as gap filler radar with pencil-beam illumination that can detect aircraft flying over wind farms without the interference from the rotating turbines.

FIG. **5** shows an example scan pattern for pencil beam gap filler radar skipping over the wind farm **550**. As can be seen, the pencil beams **500** can be directed to illuminate the blind spot area while avoiding the wind farm **550**.

Conventional radar systems use a multi-sensor multiple hypothesis tracker to merge radar data. However, this approach alone cannot avoid merging false targets from the radar data, which can result in degraded performance.

In accordance with exemplary embodiments of the invention, the inventive system merges targets that have been classified before tracking. In one embodiment shown in FIG. **6**, each radar has signal processing that includes similar processing. An airport surveillance radar **602** can include parallel data paths for a high beam receiver **604***a* and a low beam receiver **604***b*. The high and low data paths can include respective Doppler filtering **606***a,b*, CFAR detection **608***a,b* and plot extractor **610***a,b*. A classifier **612** coupled to the plot extractors **610***a,b* provides output data to a multi-sensor tracker **614** coupled to a display **616**. The gap filler radar **620** includes a receiver **622**, doppler filter **624**, CFAR detection **626**, plot extractor **628**, and classifier **630**, which provides data to the multi-sensor tracker **614**.

In general, features of each detection cluster are calculated in the plot extractor **610**, **628**, including altitude and radial velocity estimations. Outputs are then fed to the classifier **612**, **630** in each radar. The classifiers **612**, **630** should be designated for each radar since the characteristics of each radar type are unique.

In one embodiment, the classifiers **612**, **630** output the plots with confidence factors indicating the plot probabilities. The tracker **614** collects the plots from the radar systems **602**, **620** and forms tracks under the condition that the plots are classified as aircraft with a confidence factor higher than a predefined value (e.g. 0.6). If a plot is not classified as aircraft, or as a low confidence aircraft, the plot will be ignored for that scan, but may be used for coasting location update.

With the plots classified before tracking, false plots generated by the wind farm will not be treated as aircraft because of the following feature characteristics;

(1) the altitude estimation is low, (e.g., less than about 4,000 ft from local ground at about 10 nmi, and is close, (e.g., about within 0.5 nmi to known wind farm area);

(2) the estimated radial velocity does not match scan-to-scan movement;

(3) the wide Doppler spectrum, (e.g., spread over a few hundred Hertz), fits the wind turbine profile; and/or

(4) the plot is not detected by the pencil-beam gap filler radar.

In contrast, with the following feature characteristics, the radar plot of an aircraft flying over a wind farm will be classified as aircraft and continue to support the track over the wind farm:

(1) altitude estimation may drop due to the wind farm interference but is still higher than the normal wind farm altitude, (e.g., higher than about 4,000 ft from local ground at about 10 nmi); and/or

(2) the plot is detected by the pencil-beam Gap Filler radar and is classified as aircraft with high confidence factor (e.g. >0.6).

It is understood that the features used in the classifier can be provided by a variety of suitable processes and parameters, such as polarimetric characteristics, altitude estimation, detection cluster shape and size, and Doppler features. Exemplary classifier techniques are disclosed in U.S. Pat. No. 6,677,886, filed on Jan. 13, 2004, which is included herein by reference.

FIG. **7** shows an exemplary sequence of steps for implementing blind spot mitigation having target classification in accordance with exemplary embodiments of the invention. A target tracker waits in step **701** for new target plots from multiple radars. When a new target plot is received, the tracker associates the plot location to the existing track files. If the new plot is found to have range and angular location within the associated window of a track file, this new plot is assumed to be the new location of the track file in step **702**. In one embodiment, the gap-filler radar is a three dimensional radar and the fan beam radar is equipped with altitude estimation from the high and low beams, as described above. In step **704**, the system checks the altitude association and determines in step **705** if the new plot is within the altitude associated window of a track file. In step **706**, the system checks the target types between the new plot and the associated track file. If the associated track file is of the same type as determined in step **707**, the system updates the track file in step **708** with the new plot location. If any of the association process in above failed, the new plot is used for creating a new track in step **709** that includes target type and altitude.

When waiting for new plots in step **701** times out, for example, the system can examine track files in step **710**. If a track file has not been updated for the period of the longest scan time of the radars, as determined in step **711**, the track file is updated as coasting in step **712** using the predicted

location. If the track file has been coasting for N scans, as determined in step **713**, the track file is deleted in step **714**.

Exemplary embodiments of the invention merge multiple asynchronous radar data, merge radar data at target classification level, and/or merge radar data between rotating fan-beam radars and pencil-beam phase array radars. Use of the classifier output data (target type) as one of the track association parameters can significantly suppress false tracks and can maintain aircraft tracks over high clutter area.

Additional classification information is now provided. In general, method and apparatus for air clutter detection exploit weather and high/low beam target channels of a terminal S-band ASR air traffic control radar, e.g., 2700 MHZ to 2900 MHz, to create polarimetric data and altitude estimation. By also utilizing Doppler information, the system can classify detections as fixed-wing aircraft, rotary-wing aircraft, birds, insects, rain, hail, false alarms due to ground traffic, wind farm induced clutter, anomalous propagation induced clutter, and the like. In other embodiments, air clutter detection is provided as part of an en-route L-band system.

Polarimetic signatures can be used to distinguish between aircraft and birds, for example. Where a system has a target channel and a weather channel, the weather channel is a different polarization from that of the target channel, and the channels are processed in separate receiver-signal processor channels. The weather channel provides precipitation reflectivity. Using a system processor, the weather channel data is processed in a similar manner to the target channel data. The amplitude ratio and phase difference between the target and weather channel data can be calculated with the resultant amplitude-phase factors providing distinguishing target characteristics. Since the system includes high and low beams, the system can be used as in a mono-pulse radar to estimate target altitude by simultaneously processing the high and low beam data.

FIG. **8** shows an exemplary system **800** that can provide blind spot mitigation by target classification in accordance with exemplary embodiments of the invention. A pedestal **810** includes a motor **812** and encoder **814** coupled to a pedestal controller **816**. A transmitter **818** is coupled to a rotary joint **820** providing a weather channel **822** and low beam and high beam target channels **824**, **826** to an antenna assembly **828**.

The rotary joint **820** is coupled to a first RF assembly **830** and a second RF assembly **840**, each having a target low beam module **832**, **842**, a target high beam module **834**, **844**, and a weather module **836**, **846**. A first receiver/exciter **850** and a second receiver/exciter **860** each include down converter modules **852**, **854**, **856**, **862**, **864**, **866** and local oscillators **858**, **868** for the respective low beam, high beam, and weather signals. The downconverted signals are provided to first and second signal processors **870**, **880**, which are both coupled to first and second radar data processors **882**, **884** via first and second local area networks (LANs) **886**, **888**, for example.

The system **800** can include features of air traffic control systems that have an independent weather channel and target channel. Weather related false alarms in the target channel are typically not suppressed by checking against the detection of precipitation in the weather channel. Such weather channel reports are also not processed in such a manner as to be able to discern whether the precipitation type is rain, hail or snow.

The inventive system **800** uses data from both the weather high and low beam channels and target high and low beam channels to detect and classify detections for mitigating blind spots. The system takes advantage of the different polarization between the weather and the target channels to provide polarimetric data. In addition, the low and high beam of the target channels provide altitude information. Together with the Doppler and reflectivity information, the system **800** is thus capable of classifying detections and becomes an integrated detection classification system for air traffic control use.

In operation, the signal processor uses the high beam data in the short pulse range, e.g., in the order of 0.5 to 6.5 nmi to avoid the ground clutter, and switches at a predefined range, e.g., 6.5 nmi, to the low beam for complete altitude coverage.

In an exemplary embodiment, the system **800** includes a multi-channel, e.g., seven, rotary joint **820** to enable both the high beam data and the low beam data to be processed concurrently over the full instrument range. For each detection in the low beam data, the system searches for a corresponding detection in the high beam data at the same range. The altitude of the detection is estimated using a lookup table with the target amplitude ratio between the two beams as one of the indexes and the range as the other. An exemplary altitude estimation technique is shown and described by H. R. Ward in U.S. Pat. No. 4,961,075, which is incorporated herein by reference. The estimated altitude of the detection is useful for separating aircraft from false alarms due to moving clutter, such as birds, weather, etc., ground traffic and wind farms.

The system **800** also performs target detection using the weather channel data. Since the weather channel data is of a different polarization to the target channel, the differential reflectivity, differential phase and correlation coefficient between the two polarization data can be calculated. According to D. S. Zrnic, birds and insects have differential reflectivity between 2 and 9 dB and differential phase about 25 degrees; ground clutter has large differential reflectivity but has a zero mean value; weather has low differential reflectivity and phase but has high correlation coefficient. Discrimination between birds and insects is possible because insects tend to have higher differential reflectivity, while birds have higher differential phase.

FIG. **9** shows an exemplary system **900** having target classification in accordance with exemplary embodiments of the invention. The system **900** includes a high beam channel **902** and a low beam channel **904** providing data to an altitude estimation module **906**. The altitude estimation module **906** outputs altitude **908** and reflectivity **910** information to statistical classifier module **912**.

The altitude estimation module **906** provides phase information **914** to a polarimetric data module **916**, which receives data from a weather channel detection module **918** as well as reflectivity information **910** and phase information **914** from the altitude estimation module **906**. The polarimetric data module **916** provides differential reflectivity information, differential phase information, and correlation coefficient information to the statistical classifier module **912**.

In general, the polarimetric characteristics are used as detection features. Together with the estimated altitude these features are mapped to the statistics of the known detection classes, which include aircraft types, weather types, birds, insects and false alarm types. These statistics form a multi-dimensional "training database." During normal operation, the measured features are mapped to the training database to read out the detection classes. The highest class with the highest population is selected as the result and the population count is converted to a confidence factor. The confidence factors over multiple radar scans are accumulated for the detections and the conferred results are reported to the air traffic control display. The implementation of such statistical classifier could be similar to the one used in reference.

FIG. **10** shows further details **1000** of the system **900** of FIG. **9**. For the low beam target channel, data is processed by

a series of modules including a Doppler filter module **1004**, and log-magnitude calculation module **1006**. A CFAR (Constant False Alarm Rate) detection module **1008** is coupled to a binary integration module **1010**, which provides an output to an altitude estimation module **1012**. The altitude estimation module **1012** and altitude database **1014** are described more fully below.

Binary integration data (peak detection range and filter) is provided to a log-magnitude calculation module **1016** for the high beam target channel and to a module to calculate polarimetric parameters **1018**. The high beam target channel path includes a Doppler filter module **1022**, which is coupled to the log magnitude calculation module **1016**.

The low beam weather channel data is processed by a pulse compression module **1024** and a filter module **1026**. A clutter map module **1028**, a filter selection module **1030**, and a clear day coefficient selection module **1032** are coupled in parallel and exchange information with the filter module **1026**. A weather map module **1034** receives the filtered data and provides a series of outputs to a merge module **1036**, which provides output data to a weather contour module **1038** coupled to a radar data processor.

The module **1018** to calculate polarimetric parameters receives target I and Q data from the high beam target pulse compression module **1020** and weather I and Q data from the weather channel pulse compression module **1024** and generates phase and reflectivity ratio information, as described more fully below. This information is provided to a statistical target classifier module **1042**, which receives data from a trained database **1043**, outputting detection range, azimuth, altitude, target type, and confidence information provided to an RDP.

As shown in FIGS. **11** and **11**A, the high beam data and low beam data pair are extracted along with the Mode-C code. An amplitude ratio for the high and low beam data is calculated for a target range to generate an amplitude ratio table at the altitude given by the Mode-C code, as shown. In one embodiment, a 3×32 cells operator (32 range columns and 3 altitude rows) is used to average the amplitude ratio. The table is then smoothed before being used for altitude estimation. FIG. **11**A shows the smoothed amplitude ratio versus altitude curve for the range of 30 ml.

FIG. **12** shows an exemplary sequence of steps for estimating altitude in accordance with exemplary embodiments of the invention. In step **500**, the amplitude ratio is determined for a given range from the high beam signal over the low beam signal. In step **502**, it is determined whether the amplitude ratio is less than a low threshold value. If so, no estimation is performed in step **504**. If not, then it is determined in step **506** whether the amplitude ratio is greater than a high threshold. If so, no altitude estimation is performed. If not, in step **508**, the amplitude ratio is rounded to an index value. In step **510**, an altitude estimation and confidence value are generated from a table, such as the table of FIG. **12**A, from the range and index values.

In an exemplary embodiment, the target altitude is estimated at 100 foot intervals with a confidence factor ranging from 0 to 1. The confidence factor can be pre-calculated in the table based on the standard deviation of the altitude value at the given amplitude ratio before smoothing was applied, for example. It is understood that the granularity of the altitude estimate can vary to meet the needs of a particular application and the information obtainable from the radar system.

FIG. **12**A shows an exemplary plot of amplitude ratio versus altitude at various ranges, shown as 10, 20, 30, 40, and 50 nautical miles (nmi) for exemplary data. It is understood that the plotted data is smoothed. The approximate threshold values, AH and AL, are also shown marking the linear portion of the smoothed data.

FIG. **13** shows an exemplary sequence of steps for polarimetric parameter calculation in accordance with exemplary embodiments of the invention. For given range, Ic, Qc, co-polarization data, and Ir, Qr reverse polarization data, in step **1300** I and Q data is selected from the specified range R. In step **1302**, the differential reflectivity Z_{DR} is computed as

$$Z_{DR} = 10\log_{10}\left(\frac{I_C^2 + Q_C^2}{R^4}\right) - 10\log_{10}\left(\frac{I_r^2 + Q_r^2}{R^4}\right).$$

Differential reflectivity is further disclosed in U.S. Patent Publication No. 2010/0079328, filed on May 5, 2009, which is incorporated herein by reference. In step **1304**, the differential phase ϕ_{DR} is computed as

$$\phi_{DR} = \tan^{-1}\left(\frac{I_c}{Q_c}\right) - \tan^{-1}\left(\frac{I_r}{Q_r}\right).$$

FIG. **14** shows an exemplary sequence of steps for statistical target classification. In step **1400**, for given range R, estimated altitude Alt, differential reflectivity Z_{DR}, and differential phase ϕ_{DR}, integer values i_r, i_a, i_z, and i_d, are generated in step **1402** to generate probability values. More particularly, a probability of the target being an aircraft P_{tgt} is computed from a table using values tgt, i_r, i_a, i_z, i_d. In an exemplary embodiment, the indexes tgt, wx, bird and cltr represent four separate tables that form the trained database filled with measured data from known objects such as aircraft (tgt), weather (wx), birds (bird) and ground clutter (cltr). Similarly, a probability of a target being a weather-related false alarm is determined from a table based on values for wx, i_r, i_a, i_z, i_d. The probability of a target being birds is determined from bird, i_r, i_a, i_z, i_d and the probability of a target being ground clutter related false alarm is determined from cltr, i_a, i_z, i_d.

In another embodiment, the amplitude ratio (Z_{DR}) and phase difference (ϕ_{DR}) between the target and weather channel data can be calculated to distinguish target characteristics. As noted above, a DASR system, has a target and a weather channel. The weather channel is a different polarization to the target channel, and they are processed in separate receiver-signal processor channels.

The DASR weather channel determines precipitation reflectivity. In an exemplary embodiment, the weather channel data is processed in a similar manner to the target channel data. This approach provides simultaneous polarimetric data, which is an improvement over polarimetric data in alternative radar dwells. The amplitude ratio (Z_{DR}) and phase difference (ϕ_{DR}) between the target and weather channel data can be calculated as follows:

$$Z_{DR} = 10 \cdot \log_{10}\left(\frac{I_c^2 + Q_c^2}{I_r^2 + Q_r^2}\right) \quad (1)$$

$$\phi_{DR} = \tan^{-1}\left(\frac{I_c}{Q_c}\right) - \tan^{-1}\left(\frac{I_r}{Q_r}\right) \quad (2)$$

where R is range, I_c and Q_c are the in-phase and quadrature data of the co-polarization channel, and I_r and Q_r are the in-phase and quadrature data of the reverse polarization channel.

It should be noted that while some systems, such as current ASR systems use a dual fan beam, they do not provide target altitude without associated beacon data. Since a DASR has both high and low beams, these beams can be processed simultaneously in a similar manner as in a mono-pulse radar to estimate target altitude.

Actual data was recorded for simultaneous polarimetric data. FIG. **15** shows an example of estimated target altitude in comparison with the target altitude from the beacon radar. The altitude estimations (dots) have deviation from the beacon radar reported altitude (Mode Code). Smoothing the altitude estimations over 13 scans, for example, provides a more accurate estimation of the target altitude. In this case the RMS error is 240 ft.

FIG. **16** shows the distinct features of an aircraft and FIG. **17** shows possible bird data expressed in amplitude ratio versus phase difference maps based upon collected data. FIG. **16** shows the peak of the distribution at 0 degree phase difference and 6 dB amplitude ratio. The bird data in FIG. **17** has a peak of the distribution at 30 degrees phase difference and 9 dB amplitude ratio. It should be noted that the distribution in FIG. **17** has wider spread than FIG. **16**.

It is understood that a variety of polarizations can be used in various embodiments. Exemplary polarizations include linear polarization (transmission in vertical polarization, channel A received in elliptical polarization, channel B received in vertical polarization), circular polarization (transmission in circular polarization, channel A received in circular co-polarization, and channel B received in circular reverse polarization). As noted above, circular polarimetric data shows clear differences between channels and target types. It is understood that further polarization configurations are possible.

Having described exemplary embodiments of the invention, it will now become apparent to one of ordinary skill in the art that other embodiments incorporating their concepts may also be used. The embodiments contained herein should not be limited to disclosed embodiments but rather should be limited only by the spirit and scope of the appended claims. All publications and references cited herein are expressly incorporated herein by reference in their entirety.

What is claimed is:

1. A method, comprising:
employing a first radar;
identifying a blind spot in coverage of the first radar;
providing a second radar to illuminate the blind spot; and
merging data from the first and second radars using target classification prior to tracking to reduce false targets, wherein the target classification includes each of polarimetric characteristics, altitude estimation, detection cluster shape, and Doppler information.

2. The method according to claim **1**, wherein the blind spot is created by a wind farm.

3. The method according to claim **1**, wherein the first radar is an airport surveillance radar and the second radar is a gap filler radar.

4. The method according to claim **3**, wherein the gap filler radar is a pencil beam radar.

5. The method according to claim **3**, wherein the airport surveillance radar includes parallel paths for a high beam receiver and a low beam receiver.

6. The method according to claim **1**, further including identifying false targets by one or more of: an altitude estimation of a target is low and is near the blind spot, which includes a wind farm area; an estimated radial velocity of the target does not match scan-to-scan movement; a wide Doppler spectrum fits the wind turbine profile; and the target is not detected by the second radar, which is a pencil-beam gap filler radar.

7. The method according to claim **6**, further including identifying an aircraft target by detecting an altitude estimation drop due to interference by the wind farm that is higher than a predefined wind farm altitude; and/or detecting the target by the pencil-beam gap filler radar with, an aircraft classification having a confidence factor greater than and is classified as aircraft with a confidence factor greater than a selected threshold.

8. A system, comprising:
a first radar having a blind spot in coverage for the first radar;
a second radar to illuminate the blind spot; and
a tracker to merge data from the first and second radars using target classification prior to tracking to reduce false targets, wherein the target classification includes each of polarimetric characteristics, altitude estimation, detection cluster shape, and Doppler information.

9. The system according to claim **8**, wherein the blind spot is created by a wind farm.

10. The system according to claim **8**, wherein the first radar is an airport surveillance radar and the second radar is a gap filler radar.

11. The system according to claim **10**, wherein the gap filler radar is a pencil beam radar.

12. The system according to claim **10**, wherein the airport surveillance radar includes parallel paths for a high beam receiver and a low beam receiver.

13. The system according to claim **8**, wherein the tracker identifies false targets by one or more of: an altitude estimation of a target is low and is near the blind spot, which includes a wind farm area; an estimated radial velocity of the target does not match scan-to-scan movement; a wide Doppler spectrum fits the wind turbine profile; and the target is not detected by the second radar, which is a pencil-beam gap filler radar.

14. The system according to claim **13**, wherein the tracker identifies an aircraft target by detecting an altitude estimation drop due to interference by the wind farm that is higher than a predefined wind farm altitude; and/or detecting the target by the pencil-beam gap filler radar with an aircraft classification having a confidence factor greater than and is classified as aircraft with a confidence factor greater than a selected threshold.

15. A method, comprising:
employing a first radar;
identifying a blind spot in coverage of the first radar;
providing a second radar to illuminate the blind spot;
merging data from the first and second radars using target classification prior to tracking to reduce false targets;
identifying false targets by one or more of: an altitude estimation of a target is low and is near the blind, spot, which includes a wind, farm area; an estimated radial velocity of the target does not match scan-to-scan movement; a wide Doppler spectrum fits the wind turbine profile; and the target is not detected by the second radar, which is a pencil-beam gap filler radar; and
identifying an aircraft target by detecting an altitude estimation drop due to interference by the wind farm that is higher than a predefined wind farm altitude; and/or detecting the target by the pencil-beam gap filler radar with an aircraft classification having a confidence factor greater than and is classified as aircraft with a confidence factor greater than a selected threshold.

* * * * *